beta -relaxation in a simple liquid metal

1995 J. Phys.: Condens. Matter 7 1499

(http://iopscience.iop.org/0953-8984/7/8/001)

J. Phys.: Condens. Matter 7 (1995) 1499–1512. Printed in the UK

β-relaxation in a simple liquid metal

S K Lai and H C Chen

Department of Physics, National Central University, Chung-li 320, Taiwan and International Centre for Theoretical Physics, Trieste, Italy

Received 31 October 1994

Abstract. A modified hypernetted-chain theory is applied to calculate the static liquid structure factor for simple liquid metals during rapid cooling. With a proper choice of bridge function, it is found that this integral-equation theory is capable of yielding a reasonably accurate liquid structure factor in the supercooled liquid region. To exploit the usefulness of the calculated liquid structure, we combine these structure data with mode-coupling theory to investigate the dynamics of the β-relaxation process. It is demonstrated in this work that the critical temperatures for an ideal glass transition predicted here for liquid metals Na and K are slightly lower than those determined previously by us using computer-simulated structure factors. In particular, we show that the material-dependent exponent parameter λ, which is used widely in the literature as a fitting parameter in the analysis of light scattering experiments, can be given more physical significance if one correlates the change of λ with the microscopic interaction of particles specifically for the liquid metal, Lennard-Jones fluid and hard-sphere systems. The implications of the present results, and the possibility of extracting useful information for more complicated systems, is discussed in the text.

1. Introduction

The β-relaxation process for a glass-forming supercooled liquid is a subject of current interest. Empirically, this phenomenon was studied using different experimental probes. Dielectric loss spectroscopy is perhaps one of the earliest experiments that provides evidence for the existence of the β-relaxation process. Such an experimental technique was applied extensively by Goldstein and Johari [1, 2] to understand the β-resonances for a wide class of rigid molecular substances and amorphous polymers. Specifically, they observed in their measured dielectric loss spectra a secondary absorption band. To explain its origin they proposed a potential energy barrier picture, comprising cooperative and hindered types of molecular rearrangements [3, 4]. In an entirely different approach Knaak and co-workers [5] carried out an inelastic neutron scattering experiment for an ionic glass. This experiment focused on the scaling behaviour of β-resonances. The dynamics of the β-relaxation process was also investigated by Cummins and co-workers [6–10] for ionic and molecular glasses using Brillouin-scattering spectroscopy. This study was made feasible through an improved technique using the Sandercock tandem multipass Fabry–Pérot interferometer, which is an experimental setup specifically designed to circumvent the overlapping order problem. Their Brillouin spectra measurements for the dynamical structure factor exhibit a fractal law that varies as $\omega^{-(1-a)}$, where a is an exponent parameter to be defined below. In an attempt to look into the dynamical behaviour of a supercooled liquid, Pusey and Megen [11] prepared suspensions of small equal-size long-hours metastable spherical colloidal particles, and used a dynamical light scattering tool to investigate the structural and dynamical properties of the system. Because of the unique way in which the colloidal system was prepared, the

0953-8984/95/081499+14$19.50

interactions of the particles resembled that of a fluid of hard spheres, thus permitting a tractable theoretical analysis of the β-relaxation process to be made.

Theoretically, Goldstein [3] and Johari [4] attempted to interpret the β-relaxation process as originating from mobile clusters of atoms which, due to stringent atomic rearrangements, suffer the hindered type of motion for encaged atoms. However, such an idea has been questioned by Götze and Sjögren [12] as being physically unsound, since this latter feature has not been observed generally. In a series of works [12–19] Götze, Sjögren and co-workers have studied the β-relaxation process within the recently developed mode-coupling theory (MCT) of glass transitions. According to the latter works, the β-phenomenon can be understood microscopically by examining the temporal and spatial changes of the normalized intermediate scattering function $R(r, t)$. Specifically, the MCT predicts the presence of three relaxation regimes for $R(r, t)$: a microscopic relaxation time $t_0 \sim 10^{-14}$ s corresponding to uncorrelated binary collisions such as those happening in an equilibrium liquid state; an intermediate mesoscopic time t_β, typically of the order of 10^{-8}–10^{-11} s; and a long-lasting timescale $t_\alpha \sim 1$–10^3 s (the so-called α-relaxation). The β-relaxation process belongs to the mesoscopic timescales. It can be shown in the MCT that near a critical temperature, T_c, the normalized density correlation function $R(r, t)$ exhibits a factorization property which expresses $R(r, t)$ in terms of a universal temporal scaling function uncorrelated with two material-dependent spatial functions. This factorization property was investigated first for a Lennard-Jones system [20], subsequently for a hard-sphere system [17, 18, 21], and recently for a lattice gas system [22]; Cummins and co-workers [6–10] have quantitatively examined this property for the ionic and molecular glasses. In this paper we intend to supplement these works for a metallic system. Our purpose in carrying out this calculation is threefold.

First, we plan to perform a realistic calculation for the supercooled liquid metals Na and K by applying the modified hypernetted-chain integral-equation theory to the liquid structure. This recently proposed approach has been evaluated critically by us [23] to be highly reliable and accurate; it provides us with an additional channel of preparing an ideal monatomic glass which may serve the same pedagogical purpose as the computer-simulated monatomic glass. As the static liquid structure factor $S(q)$ is the sole input to MCT this application is important, not only because it offers an alternative means of calculating T_c; its comparison with T_c determined previously [24] using the molecular dynamics simulated $S(q)$ further exploits the potential of the method to an undercooled liquid. Second, we intend to compare the scaling properties of the β-relaxation process for the liquid metal, Lennard-Jones and hard-sphere systems. This comparison is instructive since it enables us to give more physical significance to the MCT exponent parameter λ (to be defined below) which has been widely used merely as a fitting parameter in experiments on glass transitions. In particular, one can infer from the variation of λ the microscopic interactions of more complex systems. Third, we shall calculate the tagged particle distribution function $P^s(r, t)$, and see if $P^s(r, t)$ for a metallic system can give any hint to the large discrepancies in this quantity between the hard-sphere and binary soft-sphere systems [18].

The format of this paper is as follows. In the next section we briefly summarize the formulae used in the modified hypernetted-chain theory, and draw attention to a bridge function that we found to yield reasonable $S(q)$. The interatomic potential used in the calculation is also outlined briefly. Section 3 is devoted to an introduction of mode-coupling theory. Here the non-linear integral equation which $R(r, t)$ satisfies will be introduced. The explicit or related expressions for the scaling formula $R(r, t)$ and for the distribution function $P^s(r, t)$ will be given in this same section. We discuss our numerical results in section 4 and give a conclusion in section 5.

2. Static structure factor

In this section we summarize essential formulae that appear in the modified hypernetted-chain theory and briefly outline the evaluation of $S(q)$.

The modified hypernetted-chain integral-equation begins with the Ornstein–Zernike relation

$$d(r) = c(r) + \rho \int \mathrm{d}r'\, d(|r - r'|)c(r') \tag{1}$$

where ρ is the number density, $c(r)$ is the direct correlation function, and $d(r) = g(r) - 1$ is the total correlation function, $g(r)$ being the pair correlation function. To solve this equation one must supplement it with a closure. The most frequently used form is

$$g(r) = \exp[d(r) - c(r) - \beta\phi(r) - B(r)] \tag{2}$$

where $\beta = (k_B T)^{-1}$ is the inverse temperature, $\phi(r)$ is the interatomic potential and $B(r)$ is the bridge function. Following our previous applications to liquid metals we construct the pair potential at each T using the modified generalized non-local model pseudopotential of Li and co-workers [25] and Wang and Lai [26]. According to the latter work $\phi(r)$ can be written

$$\phi(r) = \frac{Z_{\mathrm{eff}}^2}{r}\left(1 - \frac{2}{\pi}\int_0^\infty \mathrm{d}q\, G_{\mathrm{EC}}^{\mathrm{N}}(q)\frac{\sin qr}{q}\right) \tag{3}$$

where $G_{\mathrm{EC}}^{\mathrm{N}}(q)$ is the normalized energy-wave-number characteristic with the Singwi and co-workers [27] exchange-correlation factor included and $Z_{\mathrm{eff}}^2 = Z^2 - \rho_d^2$, Z and ρ_d being the nominal valence and depletion charges, respectively. It should be emphasized that in (3) proper attention has been given to the one-electron energy and pseudo-wavefunction by carefully incorporating higher-order perturbative corrections through a parameter in the bare-ion pseudopotential (see [25] for details). For the bridge function $B(r)$ we have chosen the empirical $B(r)$ of Malijevský and Labík [28]:

$$\sqrt{B(r)} = \begin{cases} (\nu_1 + \nu_2 y)(y - \nu_3)(y - \nu_4)/\nu_3\nu_4 & 0 \leqslant y \leqslant \nu_4 \\ \Lambda_1 \exp[-\nu_5(y - \nu_4)]\sin[\Lambda_2(y - \nu_4)]/r & y \geqslant \nu_4 \end{cases} \tag{4}$$

with $y = r/\sigma - 1$, σ being the hard-sphere diameter, and the parameters Λ_i and ν_i are determined, respectively, by continuity conditions and by fitting them to all known structural and thermodynamic computer simulation data of hard spheres over the entire fluid range up to the density of freezing. Equations (1)–(4) constitute a set of equations that are to be solved self-consistently for $g(r)$. The static structure factor $S(q)$ is then obtained by Fourier transformation.

3. Mode-coupling theory

The original derivation of the non-linear self-consistent equations has been well documented in several papers by Götze and Sjögren [29–32]. Here we review the steps that are necessary for our present purpose.

3.1. Basic formulae

Central to the MCT is the density–density correlation function $F(r,t) = \langle \delta\rho(r,t)\delta\rho(0,0)\rangle$ where $\delta\rho$(r,t) is the density fluctuation for the position vector r at time t, and $\langle\cdots\rangle$ denotes the ensemble average. According to the MCT the normalized correlator $\hat{R}(q,z) = \hat{F}(q,z)/S(q)$ satisfies

$$\hat{R}(q,z) = -\frac{z + \hat{M}(q,z)}{z^2 - q^2/m\beta S(q) + z\hat{M}(q,z)} \tag{5}$$

where m is the atomic mass and $\hat{M}(q,z)$ is the generalized frictional term, or the so-called memory function. Here the Fourier–Laplace transform of a quantity $O(q,t)$, denoted by a caret, is defined as

$$\hat{O}(q,z) = \mathrm{i}\int_0^\infty \mathrm{d}t\, \mathrm{e}^{\mathrm{i}zt} O(q,t). \tag{6}$$

Since we shall be concerned with the long-time behaviour, we make the approximation $M(q,t) \approx \Gamma(q,t)$ and ignore contributions from the transient part of $M(q,t)$; $\Gamma(q,t)$ has been derived previously by Sjögren [33] and Bengtzelius and co-workers [34] and is given by

$$\Gamma(q,t) = \frac{\rho}{8\pi^2 m\beta q}\int_0^\infty \mathrm{d}q'\, q' \int_{|q'-q|}^{|q'+q|} \mathrm{d}q''\, q''\Bigg(\frac{q'^2 - q''^2}{2q}[c(q') - c(q'')] + \tfrac{1}{2}q[c(q') + c(q'')]\Bigg)^2 S(q')S(q'')R(q',t)R(q'',t). \tag{7}$$

On the basis of many-body methods and kinetic theory, Bengtzelius and co-workers [34] successfully derived a closed non-linear self-consistent dynamical equation for the solidification:

$$\frac{f(q)}{1-f(q)} = \frac{m\beta S(q)}{q^2}\Gamma(q, t\to\infty) \equiv \mathcal{F}_q\big(f(k)\big). \tag{8}$$

In (8) the Debye–Waller form factor $f(q) = R(q, t\to\infty)$ and $\mathcal{F}_q(f(k))$ is a functional of $f(k)$ that appears in (7). Equations (7) and (8) are basic formulae, which have to be solved iteratively.

A similar equation for a tagged particle exists, and it can be written [34]

$$\frac{f^{\mathrm{s}}(q)}{1-f^{\mathrm{s}}(q)} = \frac{m\beta}{q^2}\Gamma^{\mathrm{s}}(q, t\to\infty) \equiv \mathcal{F}^{\mathrm{s}}_q\big(f^{\mathrm{s}}(k), f(k')\big) \tag{9}$$

where

$$\Gamma^{\mathrm{s}}(q,t) = \frac{\rho}{16\pi^2 m\beta q^3}\int_0^\infty \mathrm{d}q'\, q' \int_{|q-q'|}^{|q+q'|} \mathrm{d}q''\, q''[q'^2 + q^2 - q''^2]^2 c^2(q') \times S(q')R(q',t)F^{\mathrm{s}}(q'',t). \tag{10}$$

In solving for $f^{\mathrm{s}}(q)$ one requires $f(q)$ as input, but again it has to be solved self-consistently. We shall apply these equations in our calculation of the tagged particle motion.

3.2. The β-relaxation process

Following the work of Götze and Sjögren [30, 32] we present in this subsection those equations in MCT which are essential for an analysis of the β-relaxation process. The readers are referred to original papers [24, 29–32] for technical details.

According to Götze and Sjögren [30, 32] the correlator $R(q, t)$ in the vicinity of T_c can be expressed in a factorized form:

$$R(q,t) = f_c(q) + h_c(q)\mu\sqrt{1-\lambda}\sqrt{|\varepsilon|}g_{\pm}(t/t_\beta). \tag{11}$$

Here $f_c(q)$ is the Debye–Waller form factor, which is the solution of (7) and (8); $h_c(q) = [1-f_c(q)]^2 l_q^c$ is the critical amplitude [24], where l_q^c ($\hat{l}_q^c$) is the right-hand (left-hand) eigenvector of the stability matrix

$$C_{qk} = [1 - f(k)]^2 \partial \mathcal{F}_q / \partial f(k). \tag{12}$$

The term $\mu^2 = [\sum_q \hat{l}_q^c T_c (\partial \mathcal{F}_q / \partial T)_{f(k)}]/(1-\lambda)$, λ being a material-dependent exponent parameter which can be calculated from (8) [24]:

$$\lambda = \frac{1}{2} \sum_{q,k',k''} \hat{l}_q^c [1 - f(k')]^2 [\partial^2 \mathcal{F}_q / \partial f(k') \partial f(k'')]_T [1 - f(k'')]^2 l_{k'}^c l_{k''}^c. \tag{13}$$

The term $\varepsilon = (T_c - T)/T_c$ is the separation parameter, and $g_{\pm}(t/t_\beta)$ is a scaling function which satisfies

$$\mp 1 + \zeta^2 \hat{g}_{\pm}^2(\zeta) + \lambda \zeta \mathrm{i} \int_0^\infty \mathrm{d}\tau \, \mathrm{e}^{\mathrm{i}\zeta\tau} g_{\pm}^2(\tau) = 0 \tag{14}$$

where $\zeta = \omega t_\beta$ and $\tau = t/t_\beta$, both being rescaled variables. The plus and minus signs in $g_{\pm}(t/t_\beta)$ refer to glassy $\varepsilon > 0$ and liquid $\varepsilon < 0$ sides of the critical T_c, respectively. Note that the rescaled time $t_\beta = t_0 |\mu^2 (1-\lambda)\varepsilon|^{-1/(2a)}$ where the exponent parameter a can be determined from (13)

$$\lambda = \Gamma^2(1-a)/\Gamma(1-2a) \tag{15}$$

in terms of the Gamma function $\Gamma(x)$.

In the same vein the tagged particle correlator can be shown to be

$$F^s(q,t) = f_c^s(q) + h_c^s(q)\mu\sqrt{1-\lambda}\sqrt{|\varepsilon|}g_{\pm}(t/t_\beta) \tag{16}$$

where $F^s(q,t) = \langle \delta\rho^s(q,t)\delta\rho^s(0,0)\rangle$, $f_c^s(q)$ is the Lamb–Mössbauer factor, being the solution of (9) and (10), and $h_c^s(q)$ is given by [29]

$$h_c^s(q) = [1 - f_c^s(q)]^2 \sum_{k,k'} \mathcal{D}_{q,k'} [\partial \mathcal{F}_{k'}^s / \partial f(k)] h_c(k) \tag{17}$$

in which $\mathcal{D} = (\mathbf{1} - \mathbf{C}_c^s)^{-1}$ is an inverse matrix and $C_{q,k}^s = [1 - f^s(k)]^2 \partial \mathcal{F}_q^s / \partial f^s(k)$ is the tagged particle stability matrix. The above equations constitute the starting point for our discussion of the β-relaxation process.

4. Numerical results and discussion

We have applied (1)–(4) to obtain the static liquid structure factor for the liquid metals Na and K from near freezing point down to supercooled liquid temperatures. For a liquid metal these calculations pose great difficulty since the mass densities of liquid metals are *a priori* unknown. To circumvent this difficulty we resorted to our recently proposed method [24, 35] and determined this physical quantity indirectly from the simulated Wendt–Abraham parameter [36]. We refer the interested reader to these works for further details. Now, given an atomic volume at each lower T, it is then a straightforward matter to evaluate $S(q)$ [23, 37, 38]. The calculated $S(q)$ are displayed in figure 1 and they are compared with those obtained from the molecular dynamics simulation. An immediate conclusion can be drawn from this comparison: it justifies our present choice of the modified hypernetted-chain theory to the calculation of $S(q)$ for an undercooled liquid.

To proceed further we input the above $S(q)$ to (7) and (8) and iteratively solve for $f(q)$. Subsequently, the obtained solution $f(q)$ is used in conjunction with (9) and (10) to solve iteratively for the non-ergodic form factor $f^s(q)$. The critical temperatures T_c obtained for the Na and K liquid metals are $T_c = 211$ K and 194.18 K respectively. These temperatures are slightly lower than those determined previously using simulated $S(q)$ (for Na, $T_c = 215.78$ K; for K, $T_c = 200.2$ K). The difference, apart from the numerical uncertainties inherent in the MD $g(r)$ (see the discussion on p 4332 in [24]), can be understood to be partly due to the use of the short-range hard-sphere bridge function (to be compared with a metallic $B(r)$ to which corresponds the MD-based $g(r)$) which generally yields a slightly different structure in the second maximum of $S(q)$ (see figure 3(*a*) in [23]). In the following, we present and discuss some interesting results.

Table 1. The parameters λ and a calculated from the present work, and the characteristic time t_β scaled by the microscopic time t_0 for the liquid metals Na and K compared with those of the hard-sphere (HS) calculated using the Malijevský and Labík [28] bridge function at the critical packing ratio 0.5324 and the Lennard-Jones (LJ) [20] systems.

System	λ	a	$t_\beta/t_0 \times 10^{-4}$
HS	0.772	0.294	6.16
LJ	0.714	0.321	—
Na	0.712	0.322	—
K	0.710	0.323	20.71

4.1. Exponent parameter λ

Using (13) we have calculated the exponent parameter λ and hence the parameter a from (15). These exponent parameters are given in table 1 along with those corresponding to the HS calculated using the empirical $B(r)$ given by (4) and the Lennard-Jones [20] system. A notable feature in this table is that λ shows a systematic change; it decreases from a large value of 0.772† for hard spheres (characterized by a purely infinite repulsive part), to a value of 0.714 for a Lennard-Jones system (delineated by a still highly repulsive part but a weakly attractive part), and to values of 0.712 and 0.710 for liquid metals (described

† This λ is larger than 0.758 obtained previously [21] using the Verlet–Weis–Henderson–Grundke [39, 40] structure factor. The discrepancy lies in the presently employed $S(q)$ which was demonstrated by Labík and Malijevský [41] to be a more accurate description of the hard-sphere system (see figure 1 in this reference).

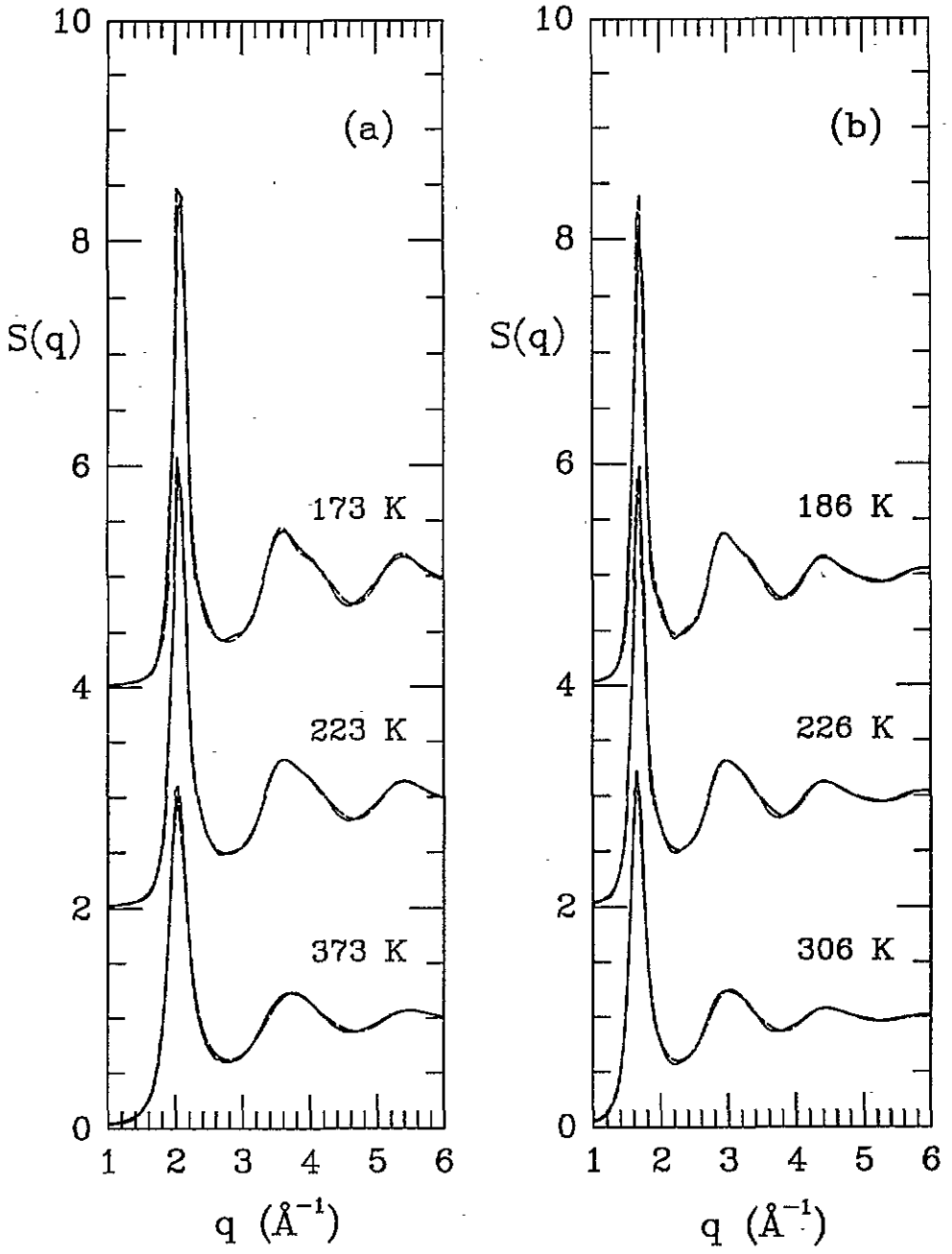

Figure 1. Static liquid structure factor $S(q)$ calculated using the modified hypernetted-chain theory (broken curve) with the Malijevský and Labík empirical bridge function [28] compared with the Fourier-transformed molecular dynamics $g(r)$ (full curve) for (a) sodium and (b) potassium liquid metals.

by a relatively softer repulsive part followed by an oscillatory weakly attractive part). This variation of λ is surely intimately related to the details of microscopic interactions. In fact, it is possible to infer from this change of λ that for a simple monatomic system such as

the one-component plasma (having a much softer repulsive part and a zero attractive part), it will be expected to have an exponent parameter that lies within the range $0.772 \geqslant \lambda \geqslant 0.714$. This prediction is based on the assumption that the attractive part of the pair potential does play some role in the dynamics of liquid structure, and that the Lennard-Jones system has a sufficiently weak attractive tail. It would be interesting to carry out such a calculation to check this conjecture.

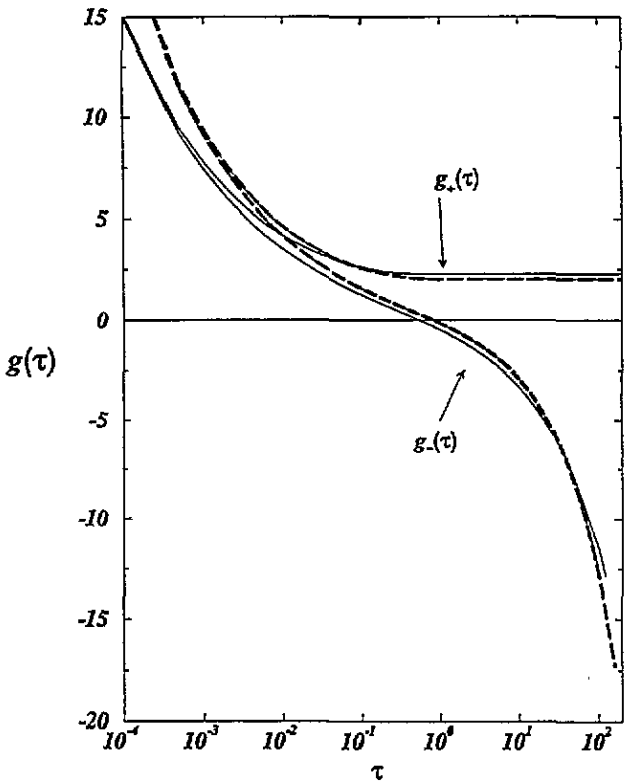

Figure 2. Master function $g_{\pm}(\tau)$ against $\tau = t/t_{\beta}$ for the hard-sphere system (full curve) and liquid metals Na (light broken curve) and K (heavy broken curve).

4.2. Master function for the β-relaxation

From the λ given above, it is numerically straightforward to calculate the master functions $g_{\pm}(\tau)$ [16]†. They are given in figure 2 for the hard-sphere (HS) and liquid metals Na and K. However, the calculated results are equally instructive if they are expressed in their Laplace transform $\hat{g}_{\pm}(z)$. For real frequencies ω, $z \to \omega + \mathrm{i}0$, one obtains

$$\hat{g}_{\pm}(\omega + \mathrm{i}0) = \mathrm{i}\int_0^{\infty} g_{\pm}(t)\cos(\omega t)\,\mathrm{d}t - \int_0^{\infty} g_{\pm}(t)\sin(\omega t)\,\mathrm{d}t = \mathrm{i}\hat{g}''_{\pm}(\omega) - \hat{g}'_{\pm}(\omega)$$

† In consulting [16] for the numerical treatment of the singular part, care must be exercised in directly applying the algorithm, especially on p 8489.

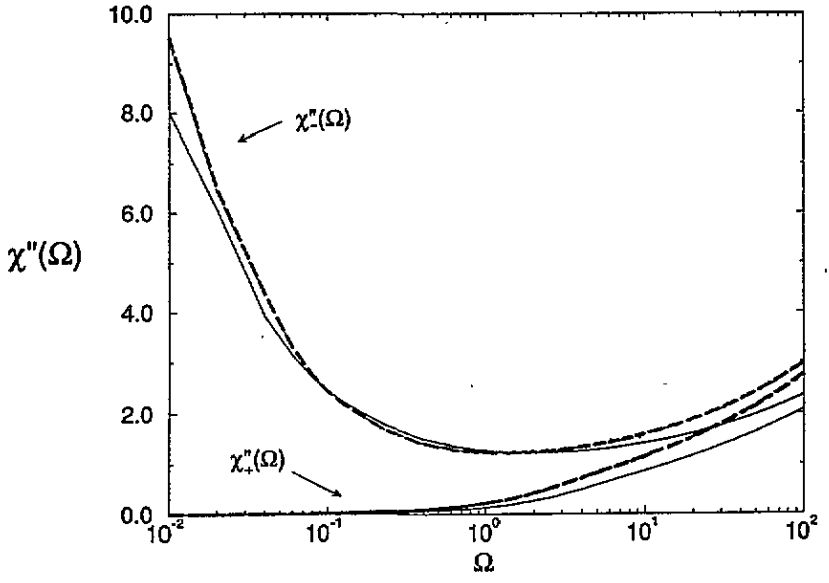

Figure 3. Susceptibility spectra $\chi''(\Omega)$ against $\Omega = \omega/\omega_\beta$ (where $\omega_\beta = 1/t_\beta$) for the hard-sphere system (full curve) and liquid metals Na (light broken curve) and K (heavy broken curve).

and the corresponding susceptibility spectra $\chi_\pm(\omega)$ can be calculated from $\chi_\pm(\omega) = \omega\hat{g}_\pm(\omega)$. The $\chi''_\pm(\omega)$ for liquid metals Na and K are depicted in figure 3, together with that for the HS system included for comparison. It is interesting to note the following discernible differences.

(i) For a given ε, the master function $g_\pm(\tau)$ for a metallic system varies more steeply with τ for $\tau \ll 1$ and $\tau \gg 1$ compared with that for hard-spheres.

(ii) The susceptibility spectra $\chi''_-(\omega)$ for the HS system has a broader dispersion relative to those of liquid metals Na and K.

These two points, the validity of one which implies the validity of the other, can be understood qualitatively by examining the details of interactions between particles. For HS we note that the *microscopic interaction* is purely geometrical, being characterized by an infinite repulsive potential. The structural behaviour is therefore determined solely by the excluded volume effect. On the other hand, the microscopic interaction of a liquid metal is described by a relatively soft finite repulsive force embellished by an oscillatory weakly attractive part. Thus the structural behaviour is determined both by the geometrical factor, similar in nature to that of a HS system, and by an additional Coulomb attraction due to the presence of valence electrons. When the temperature (density) of an equilibrium liquid is rapidly decreased (increased) it is anticipated that the non-linear coupling between particles is enhanced by the attractive force that prevails in a metallic system. Since the β-relaxation process is believed to be a localized excitation, describing particles moving dynamically with their surrounding cages, such an enhancement in the attractive interaction with decreasing temperature (or increasing density) has the consequence of making more robust the occurrence of the β-relaxation process, as evidenced by a longer characteristic timescale t_β for the liquid metal than for the HS system (see table 1). This would imply that the atomic motion in its associated cage is relatively more stable for a metallic atom

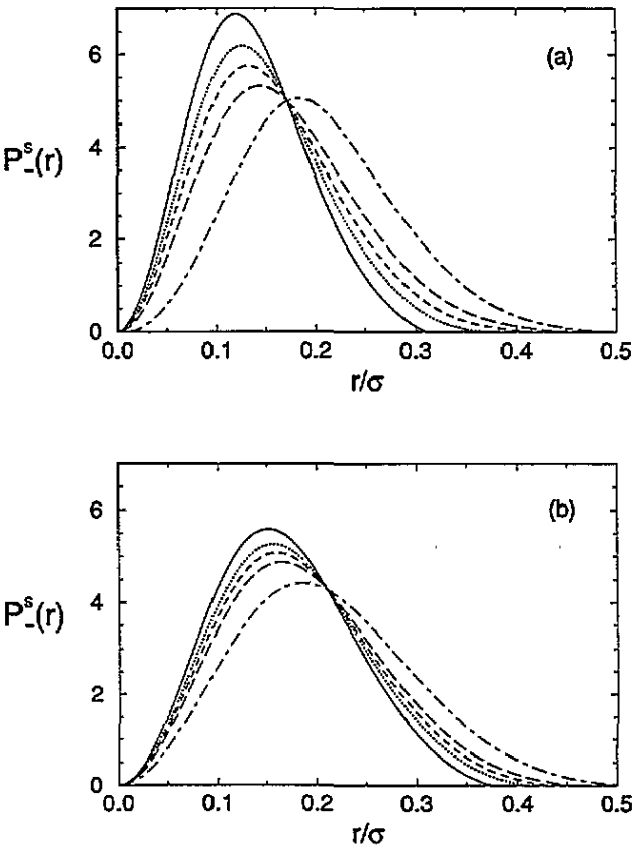

Figure 4. Tagged particle distribution function $P^s_-(r)$ for (a) hard spheres and (b) the potassium element evaluated at $\tau_i/t_\beta = 5\times10^{-3}$ (full curve), 5×10^{-2} (dotted curve), 5×10^{-1} (short-dash broken curve), 5×10^{0} (long-dash broken curve), and 5×10^{1} (chain curve) for the $\varepsilon < 0$ liquid region.

than for a HS particle. We will see more clearly such a picture below, when we discuss the tagged particle distribution function.

Before proceeding to the latter discussion, we should mention one interesting aspect of figure 3. This figure reminds us of recent theoretical fittings of the MCT to light scattering experiments on $Ca_{0.4}K_{0.6}(NO_3)_{1.4}$ [8–10]. There, the fitted values $\lambda = 0.81$–0.85 surely imply that the details of inter-particle interactions should differ considerably from the presently considered monatomic systems. Indeed, for this particular fragile glass, which consists of argon-like ions K^+ and Ca^+, and optically anisotropic ions $(NO_3)^-$, it is believed that the orientational motion of the planar $(NO_3)^-$ is probably the most relevant cause of the distinctly large value of λ.

4.3. Tagged particle distribution function

We turn now to a discussion of the tagged particle distribution function $P^s(r,t) = 4\pi r^2 F^s(r,t)$, which can be obtained from (16) by a back Fourier transformation. This equation, which is

$$P^s_\pm(r,t) = p^s_c(r) + H^s_c(r)\mu\sqrt{1-\lambda}\sqrt{|\varepsilon|}g_\pm(t/t_\beta) \tag{18}$$

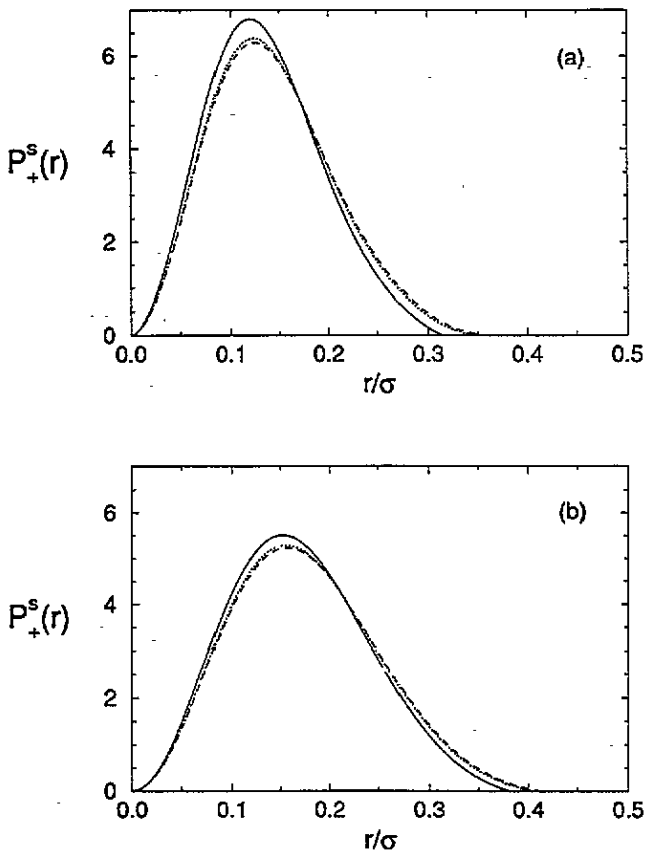

Figure 5. Tagged particle distribution function $P^s_+(r)$ for (a) hard spheres and (b) the potassium element evaluated at $\tau_i/t_\beta = 10^{-2}$ (full curve), 10^{-1} (dotted curve), and 10^0 (broken curve) for the $\varepsilon > 0$ glassy region.

describes the probability density of locating a tagged particle at time t and position r, if it was found to appear at the origin $r = 0$ at $t = 0$. Figures 4 and 5 display the $P^s_\mp(r, \tau = t/t_\beta)$ against r/σ for the liquid metal K and HS system calculated using the $g_-(\tau)$ and $g_+(\tau)$ respectively. (The result for the liquid metal Na is virtually the same and is therefore not given here). There are two interesting points that merit emphasis.

(i) For a given $\varepsilon < 0$, the HS tagged particle $P^s(r, \tau)$ at different τ intercepts at $r/\sigma = 0.172$ (for K, $r/\sigma = 0.211$). Since the probability of finding the HS tagged particle is higher for increasing τ for $r/\sigma > 0.172$ (for K, $r/\sigma > 0.211$), the HS tagged particle is seen to push its way through the cage of neighbouring particles. Such a picture for atomic motion in a cluster of particles appears to persist longer for a metallic atom than for a HS particle.

(ii) For a given $\varepsilon > 0$, the tagged particle $P^s(r, \tau)$ at different τ displays the characteristic localized motion and shows a slightly more stable configuration for metallic particles than HS particles.

The first point can be explained by referring to the master function given in figure 2. There we see that the metallic $g_-(\tau)$ lies above that of HS throughout the time window of the β-relaxation process. Further evidence for this difference in the diffusive motion can also

Table 2. Tagged particle distribution function $P^s(r_{max}, \tau_i)$ evaluated at the maximum position r_{max} for $\tau_i = t_i/t_\beta = 5 \times 10^{-3+i}$ where $i = 0, \ldots, 4$ for the HS and liquid metal K in the $\varepsilon < 0$ liquid region. In the $\varepsilon > 0$ glassy region $\tau_{l+4} = t_{l+4}/t_\beta = 10^{-3+l}$ where $l = 1, \ldots, 3$.

	τ_0	τ_1	τ_2	τ_3	τ_4	τ_5	τ_6	τ_7
HS system								
r_{max}/σ	0.120	0.126	0.132	0.144	0.184	0.120	0.124	0.125
$P^s(r_{max}, \tau_i)$	6.876	6.181	5.751	5.309	5.044	6.804	6.379	6.289
K system								
r_{max}/σ	0.152	0.157	0.159	0.164	0.187	0.152	0.157	0.159
$P^s(r_{max}, \tau_i)$	5.582	5.252	5.066	4.867	4.409	5.507	5.289	5.229

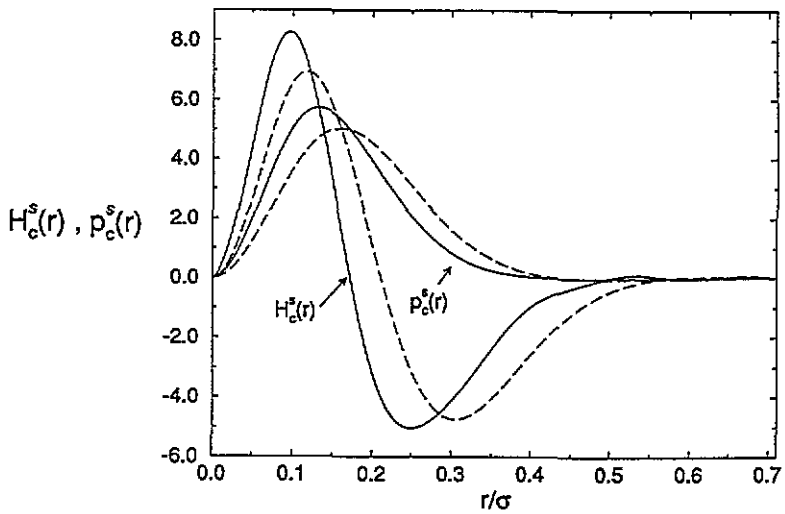

Figure 6. Spatial functions $H_c^s(r)$ and $p_c^s(r)$ for the tagged particle distribution for the hard-sphere system (full curve) and liquid metal K (broken curve).

be gleaned from table 2, where we give the $P^s(r_{max}, \tau)$ at the maximum position r_{max} for increasing τ. As regards the second point, it can be attributed physically to the attractive part of ϕ(r) being more important when the system is at a lower (higher) temperature (density).

Finally, it is of great theoretical interest to compare our calculated monatomic metallic $H_c^s(r)$ with that of the computer simulated soft-sphere mixture (see figure 1 in [18]). Our metallic H_c^s(r) shows the same peak–valley behaviour as that of HS. Quantitatively, however, the magnitude of the first peak is lower and the whole curve is shifted to larger r-values (see figure 6). This latter feature is qualitatively similar to the soft-sphere mixture and may be attributed to the more realistic repulsiveness of $\phi(r)$. A comparison between the present result for K and the soft-sphere mixture further implies that the single-peak feature, followed by an extensive spatial $H_c^s(r)$ for the latter, might be due to the size effect of different soft spheres.

5. Conclusion

In this paper we first examined the appropriateness of the modified hypernetted-chain theory

when applied to the evaluation of the static liquid structure factor for an undercooled liquid. We compared the calculated liquid structure factor with MD simulated $S(q)$ and found that they agree very well for the supercooled liquid region of interest in this work. This prompted us to apply the calculated $S(q)$ in conjunction with mode-coupling theory to study the β-relaxation process. We chose liquid metal as a prototype system, since it is described by the simplest realistic interactions which, when compared with the HS and Lennard-Jones systems, permits extraction of fruitful information about the supercooled liquid dynamics. It was further attempted in this work to establish the connection between the details of microscopic interactions and the parameters that appear in mode-coupling theory. For simple monatomic systems, we found that the strength of the attractive part of the pair potential (i) varies inversely with the λ parameter and (ii) makes more robust the occurrence of β-relaxation process, and hence has the tendency of stabilizing the motion of the tagged particle in its neighbourhood.

Acknowledgments

This work was supported in part by the National Science Council, Taiwan under contract No NSC83-0208-M008-056. We thank the Computer Centre of the Department of Physics, National Central University (NSC82-0208-M008-094) for the support of computing facilities. One of the authors (SKL) would like to thank Professor Abdus Salam, the International Atomic Energy Agency and UNESCO for hospitality at the International Centre for Theoretical Physics, Trieste, Italy.

References

[1] Johari G P and Goldstein M 1970 *J. Phys. Chem.* **74** 2034
[2] Johari G P and Goldstein M 1970 *J. Chem. Phys.* **53** 2372
[3] Goldstein M 1969 *J. Chem. Phys.* **51** 3728
[4] Johari G P 1973 *J. Chem. Phys.* **58** 1766
[5] Knaak W, Mezei F and Farago B 1988 *Europhys. Lett.* **7** 529
[6] Tao N J, Li G and Cummins H Z 1991 *Phys. Rev. Lett.* **66** 1334
[7] Li G, Du W M, Sakai A and Cummins H Z 1992 *Phys. Rev.* A **46** 3343
[8] Li G, Du W M, Chen X K and Cummins H Z 1992 *Phys. Rev.* A **45** 3867
[9] Li G, Du W M, Hernandez J and Cummins H Z 1993 *Phys. Rev.* E **48** 1192
[10] Cummins H Z, Du W M, Fuchs M, Götze W, Hilderbrand S, Latz A, Li G and Tao N J 1993 *Phys. Rev.* E **47** 4223
[11] Pusey P N and van Megen W 1987 *Phys. Rev.* A **59** 2083
[12] Götze W and Sjögren L 1991 *J. Non-Cryst. Solids* **131–3** 161
[13] Götze W and Sjögren L 1988 *J. Phys. C: Solid State Phys.* **21** 3407
[14] Buchalla G, Dersch U, Götze W and Sjögren L 1988 *J. Phys. C: Solid State Phys.* **21** 4239
[15] Götze W and Sjögren L 1989 *J. Phys.: Condens. Matter* **1** 4183
[16] Götze W 1990 *J. Phys.: Condens. Matter* **2** 8485
[17] Götze W and Sjögren L 1991 *Phys. Rev.* A **43** 5442
[18] Fuchs M, Götze W, Hilderbrand S and Latz A 1992 *Z. Phys.* **87** 43
[19] Fuchs M, Götze W, Hilderbrand S and Latz A 1992 *J. Phys.: Condens. Matter* **4** 7709
[20] Bengtzelius U 1986 *Phys. Rev.* A **34** 5059
[21] Barrat J L, Götze W and Latz A 1989 *J. Phys.: Condens. Matter* **1** 7163
[22] Knob W and Andersen H C 1993 *Phys. Rev.* E **47** 3281
[23] Chen H C and Lai S K 1994 *Phys. Rev.* E **49** R982
[24] Lai S K and Chen H C 1993 *J. Phys.: Condens. Matter* **5** 4325
[25] Li D H, Li X R and Wang S 1986 *J. Phys. F: Met. Phys.* **16** 309
[26] Wang S and Lai S K 1980 *J. Phys. F: Met. Phys.* **10** 2717

[27] Singwi K S, Sjölander A, Tosi M P and Land R H 1970 *Phys. Rev.* **B 1** 1044
[28] Malijevský A and Labík S 1987 *Mol. Phys.* **67** 663
[29] Götze W 1985 *Z. Phys.* **60** 195
[30] Götze W 1991 *Liquids, Freezing and the Glass Transition* ed J P Hansen, D Levesque and J Zinn-Justin (Amsterdam: North Holland) p 287
[31] Götze W 1987 *Amorphous and Liquid Materials* ed E Lüscher, G Fritsch and G Jacucci (Dordrecht: Martinus Nijhoff) p 34
[32] Götze W and Sjögren L 1992 *Rep. Prog. Phys.* **55** 241
[33] Sjögren 1980 *Phys. Rev.* A **22** 2883
[34] Bengtzelius U, Götze W and Sjölander A 1984 *J. Phys. C: Solid State Phys.* **17** 5915
[35] Lai S K, Chou M H and Chen H C 1993 *Phys. Rev.* E **48** 214
[36] Wendt H R and Abraham F F 1978 *Phys. Rev. Lett.* **41** 1244
Abraham F F 1980 *J. Chem. Phys.* **72** 359
[37] Lai S K, Wang Li and Tosi M P 1990 *Phys. Rev.* A **42** 7289
[38] Chen H C and Lai S K 1992 *Phys. Rev.* A **45** 3831
[39] Verlet L and Weis J J 1972 *Phys. Rev.* A **5** 939
[40] Henderson D and Grundke E W 1975 *J. Chem. Phys.* **63** 601
[41] Labík S and Malijevský A 1989 *Mol. Phys.* **67** 431